Original

Morphometrical, Histological and Ultrastructural Analyses of Bone Formation and Resorption Induced by Synthetic Octacalcium Phosphate in Mouse Bone Marrow

Yoshitaka NAGAI*,**, Mitsuori MAYAHARA***, Osamu SUZUKI****, Hisashi HISAMITSU** and Masanori NAKAMURA*

*Department of Oral Anatomy and Developmental Biology, Showa University School of Dentistry
1–5–8 Hatanodai, Shinagawa-ku, Tokyo, 142–8555 Japan
(Chief: Prof. Masanori Nakamura)
**Department of Clinica Cariology and Endodontology, Showa University School of Dentistry
2–1–1 Kitasenzoku, Ohta-ku, Tokyo, 145–8515 Japan
(Chief: Prof. Hisashi Hisamitsu)
***Department of Oral Histology, Showa University School of Dentistry
1–5–8 Hatanodai, Shinagawa-ku, Tokyo, 142–8555 Japan
****Division of Craniofacial Function Engineering, Tohoku University Graduate School of Dentistry
4–1 Seiryo-machi, Aoba-ku, Sendai, Miyagi, 980–8575 Japan
(Chief: Prof. Osamu Suzuki)

Abstract: *Objective:* Octacalcium phosphate (OCP) is thought to be a precursor of the mineral crystals in biological apatite. Synthetic OCP has been shown to be converted into an apatite structure when implanted in murine calvarial bone, to enhance bone regeneration.This study was designed to investigate whether OCP implantation enhances the formation and resorption of new bone when implanted intramedullary in a mouse bone marrow.

Design: Histological and ultrastructural analyses of bone formation and resorption after 2, 4 and 6 weeks implantation was investigated. MicroCT analysis was also applied to detect the amount of newly formed bone mass after implantation.

Results: Massive bone formation on OCP was detected at 2 weeks. Then, the amount of bone was decreased gradually until 6 weeks. At 4 and 6 weeks, many multinucleated giant cells, including tartrate-resistant acid phosphatase (TRAP)-positive cells, were detected on the newly formed bone and synthetic OCP. Ultrastructural study indicated that the multinucleated giant cells attached either to the bone and OCP surface were osteoclasts forming the clear zones and ruffled borders composed of finger-type and plate-type cell processes. However, the ultrastructure of cell processes in ruffled borders showed the irregular shape. No representative cell processes were detected in the cells.

Conclusion: These results confirmed the active induction of bone formation and resorption on OCP and also suggested that the structure of ruffled border might be regulated by the target calcified materials.

Key words: octacalcium phosphate, bone regeneration, osteoclast, biomaterials.

The mineral in bones and teeth is basic calcium phosphate hydroxyapatite [$Ca_{10}(PO_4)_6(OH)_2$, HA], containing impurities such as carbonate and structural defects.[1~3] Octacalcium phosphate [$Ca_8H_2(PO_4)_6 \cdot 5H_2O$, OCP] is thought to be a precursor of biological apatite crystals in bone, dentin and cementum.[4~8] Although there is still controversy over whether OCP precipitates before the formation of HA,[9] the existence of an OCP precursor would explain the nonstoichiometry of mineral crystal composition.[10,11] Synthetic HA and β-tricalcium phosphate [$Ca_3(PO_4)_2$, β-TCP] bone substitutes have been used for orthopedic, trau-

(Received December 9, 2009; Accepted for publication December 15, 2009)

matological, and odontological surgery and recognized as biocompatible and osteoconductive,[12, 13] and β-TCP is also bioresorbable.[12~14]

Synthetic OCP exhibit conversion into an apatite structure *in vivo*, biodegrade faster than β-TCP ceramic, and enhance bone formation more than HA and β-TCP ceramic when implanted in rat calvaria.[15] The biodegradation of Ca-P biomaterials is generally assumed to take place by solution-driven and to be influenced by the experimental conditions, such as experimental models, implantation sites, and animal species.[16] OCP is a salt that is more soluble than β-TCP and HA at physiological pH and thermodynamically favored to convert into HA.[17] Ca-P ceramic biodegradation is highest in marrow tissue and higher in cancellous bone than cortical bone; hence, marrow tissue was suggested to be better for testing material biocompatibility *in vivo*.[18] Experimentally induced bone tissues could be resorbed over time in the bone marrow by cooperation between osteoblasts and osteoclasts.

In this study, we designed the experiments to examine the process of bone regeneration and biodegradation of newly formed bone on OCP and to identify the cells resorbing directly OCP.

Materials and Methods

Animals and reagents

Specific pathogen-free male ICR mice (6 weeks old) were purchased from Saitama Breeding Laboratory (Saitama, Japan) and maintained under routine conditions at the Laboratory Animal Center of Showa University. The experimental protocol was approved by the animal care committee of Showa University.

Materials

OCP was prepared according to the method described by LeGeros.[19] Ground granules of between 16 and 32 mesh (particle size 0.5～1.0 mm) were used for implantation. The sieved granules were sterilized by heating at 120°C for 2 h. Our previous studies showed that such heating does not affect physical properties such as the crystalline structure or specific surface area of OCP granules.[20, 21] The crystalline structures of OCP was characterized by X-ray diffraction (XRD). Powder XRD patterns of ground OCP were obtained by a scanning step with Cu Ka X-rays on a Rigaku Electrical (Tokyo, Japan) RAD-2B diffractometer at 40 KV, 20 mA. The morphology of each granule was observed by scanning electron microscopy (SEM).

Implantation of OCP into the bone marrow

Mice were anesthetized with ether. Lateral incisions of 0.5 mm were made aseptically along the medial side of the tibia, and standardized defects, 1.5 mm in diameter, were made in the cortex of the metaphysis of tibia using a surgical drill. After the defects were thoroughly washed by saline solution, 15 pieces of OCP were implanted into the bone marrow space of the tibia. Five mice were killed by cervical dislocation at 2, 4 and 6 weeks after implantation.

Tissue preparation for histological and histochemical detection

Tibias were dissected and fixed with 4% paraformaldehyde in PBS. After the decalcification with 10% EDTA, specimens were dehydrated with graded series of ethanol, passed through xylene and embedded in paraffin. Five micrometer thick sections were stained with Hematoxylin and Eosin. Some of the sections were processed for the detection of tartrate-resistant acid phosphatase activities by azo staining using naphthol AS-BI phosphate coupled with fast red violet LB salt.

Tissue preparation for transmission electron microscopy

Tibias were fixed with the mixture of 2% paraformaldehyde and 2.5% glutaraldehyde in 0.1 M sodium cacodylate buffer (pH 7.4). After demineralization with or without 10% EDTA, specimens were post-fixed with 2% osmium tetroxide, dehydrated by a graded series of ethanol, passed through propylene oxide and embedded in EPON 812. Ultra-thin sections were stained with uranyl acetate and lead citrate and examined with a HITACHI H-7000 transmission electron microscope.

Microcomputed tomography (MicroCT) analysis

Paraformaldehyde-fixed tibias were immersed in saline solution. Parameters of volume, architecture, and percentage of OCP injection surface in direct

contact with trabecular bone were studied using CT morphometry (SMX90CT ; Shimadzu Co., Kyoto, Japan). The voxel was 15 μm in all spatial directions. The system was set to 90 kEV and 110 mA. The number of tomographic projections was 1200 projections per 360°. Volume analysis of the data was performed using a 3-D construction imaging system (TRI, RATOC System Engineering, Tokyo, Japan). Trabecular bone was analyzed on a circular band of longitudinal both 1.5 mm (Fig. 1) by an OCP injection part. The bone marrow cavity volume assumed (TV), a trabecular bone volume (BV). These relative bone volume was (BV/TV), were calculated by measuring direct 3D distance with trabecular meshwork.

Statistical analysis

All the samples were expressed as mean ±standard deviation (SD). These relative bone volume was (BV/TV), were calculated by measuring direct 3D distance with trabecular meshwork. All statistical analyses used ANOVA and Tukey's post hoc tests (= 0.05, n = 3). A significance level of $p < 0.05$ was set for all the comparisons.

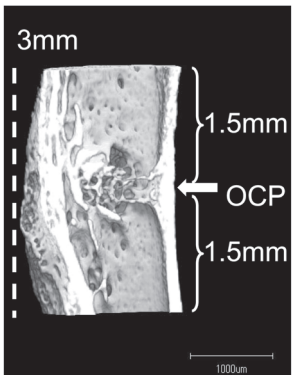

Fig. 1 Analyzed area of Tibia by microCT. Trabecular bone was analyzed on a circular band of longitudinal both 1.5 mm by an OCP injection part.

Results

MicroCT analysis of bone regeneration by OCP implantation

MicroCT indicated the bone formation at 2 weeks after OCP implantation in the bone marrow (Fig. 2a). At 4 and 6 weeks, these trabecular bones were gradually decreased (Fig. 2b, c). Tibial BV/TV at 2 weeks after the implantation was over 16.6±0.9 (%), and then decreased to 13.5±0.3 and 13.0±0.4 at 4 and 6 weeks, respectively. A significant difference was present for 4 weeks and 6 weeks in comparison with 2 weeks. Bone marrow cavity volume 3.5±0.1(mm^3) are 2.6±0.6, 2.9±0.5, and there is not a significant difference with all groups. Therefore, a significant difference in (BV/TV) shows decrease of quantity of trabecular bone (Table 1).

Histologial observation of bone formation

Most of implanted OCP was surrounded by newly formed bone by osteoblasts at 2 weeks after the implantation (Fig. 3a). Many osteoblasts were aligned on the bone surface while osteoclasts were not easily detected at this stage (Fig. 3d). As indicated by

Table 1 Bone marrow cavity volume (TV), trabecular bone volume (BV), relative bone volume (BV/TV) after OCP implantation.

Weeks	BV/TV (%)	BV (mm^3)	TV (mm^3)
2W	16.6±0.9	0.59±0.01	3.5±0.1
4W	13.5±0.3*	0.3 ±0.08	2.6±0.6
6W	13.0±0.4*	0.39±0.08	2.9±0.5

*$p < 0.05$

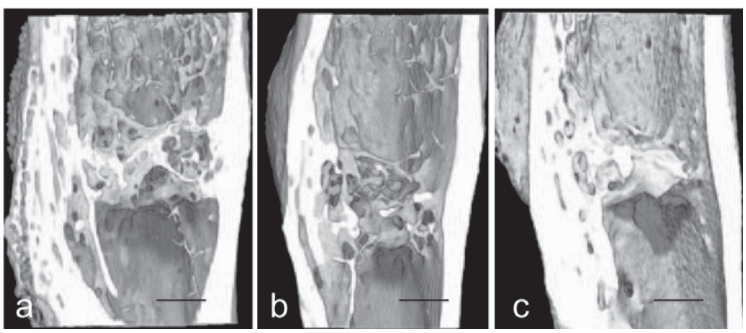

Fig. 2 Detection of trabecular bone formation in the bone marrow by microCT at 2 (a), 4 (b) and 6 (c) weeks after OCP implantation. Trabecular bones were colored by yellow. Scale bar = 500 μm.

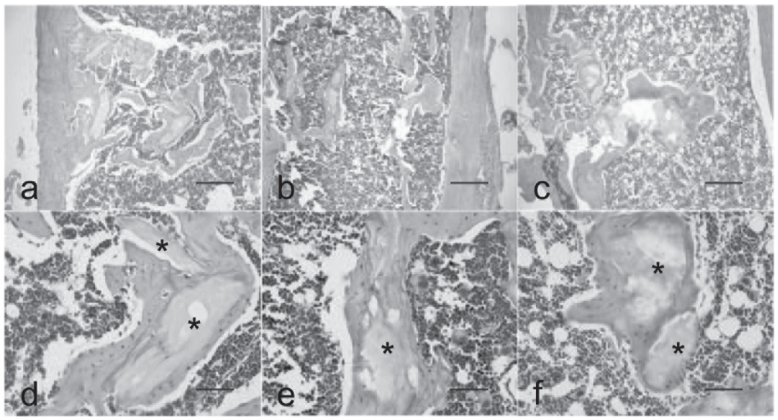

Fig. 3 Hematoxylin-Eosin staining of trabecular bones at 2 (a, d), 4 (b, e) and 6 (c, f) weeks after OCP implantation. * indicated implanted OCP. Scale bar = 250, 50 μm.

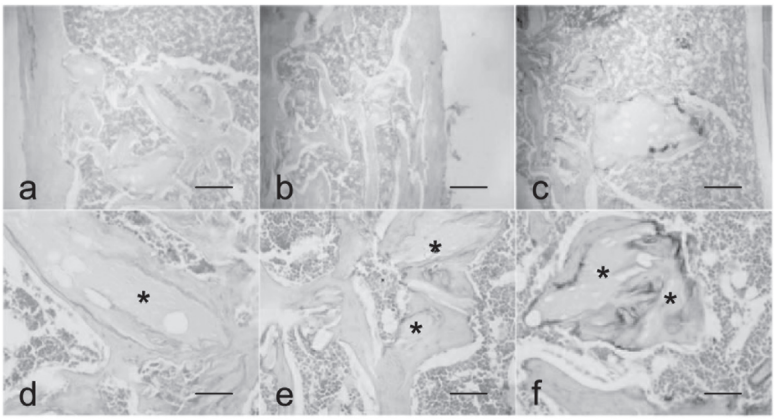

Fig. 4 TRAP staining of trabecular bones at 2 (a, d), 4 (b, e) and 6 (c, f) weeks after OCP implantation. Strong reactions were detected on the newly formed bone and COP at 6 weeks. * indicated implanted OCP. Scale bar = 250, 50 μm.

microCT analysis, the number of trabecular bone was decreased at 4 weeks (Fig. 3b, e) and a few of the trabecular bone were only detected at 6 weeks (Fig. 3c, f). A small number of osteoclasts was observed on the bone surface at 4 weeks (Fig. 3e) and easily detected at 6 weeks (Fig. 3f).

Detection of TRAP positive cells

At 2 weeks, almost no TRAP positive cells were detected on the bone surface (Fig. 4a, d). TRAP positive cells were recognized on the bone surface at 4 weeks (Fig. 4b, e). AT 6 weeks, many TRAP positive cells were detected on the bone surface (Fig. 4c, f).

Ultrastructural detection of osteoclasts

Osteoclasts attached on the surface of newly formed bone showed well developed clear zones and the ruffled border (Fig. 5a, b). Cell projections of the ruffled border composed of finger-type and plate-type processes (Fig. 5b). The coarse distribution of collagen fibers was detected in the bone matrix adjacent to the ruffled border, which indicated the active bone resorption by osteoclasts (Fig. 5b).

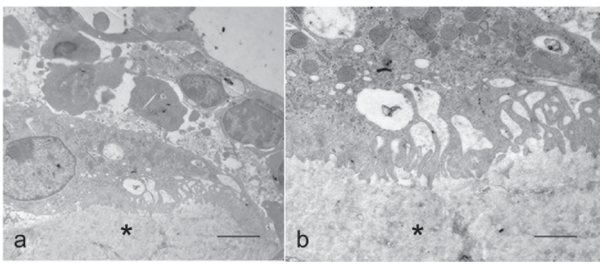

Fig. 5 Osteoclasts resorbing nearly formed bone (*) at 4 weeks after OCP implantation. (a) Osteoclast attached on the bone surface by clear zone and resorbed bone by ruffled border. (b) Finger-shaped and plate-shaped cell processes were detected in the ruffled boder. Scale bar = 5 microns.

Multinucleated giant cells were attached on the surface of implanted OCP (Fig. 6a, b). Nuclei of the cells were located at the site opposite to the implanted OCP and great numbers of mitochondria were located within the cytoplasm (Fig. 6a, b). These cells attached on implanted OCP by clear zones and extended a number of cell processes of the ruffled border to the

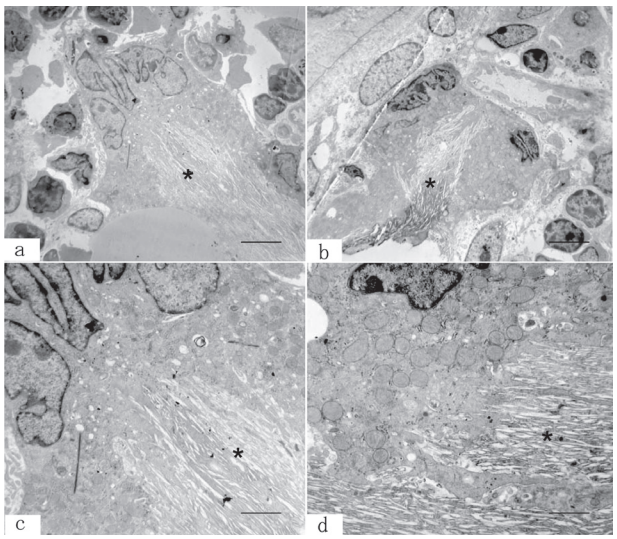

Fig. 6 Osteoclasts resorbing implanted OCP (*) at 4 weeks after OCP implantation. (a, b) Multinucleated cells were attached on the surface of OCP by clear zone and resorbed OCP by ruffled border. (c, d) Cell processes in the ruffled border showed the irregular shape. The implanted OCP facing the ruffled border was frayed and decreased the electron-dense intensity. Scale bar = 5 microns.

resorption pit (Fig. 6a, b). The ultrastructure of the processes showed the irregular shape, which was quit different from the processes of osteoclasts resorbing bone (Fig. 6c, d). Electron-dense substances were deposited on the surface of electron-lucent OCP crystals (Fig. 6c, d). The OCP adjacent to the ruffled border showed frayed and decreased the electron-dense intensity (Fig. 5c, d).

Discussion

This study showed the osteogenic characteristics of synthetic OCP when implanted in mouse bone marrow. The marrow space is a site where Ca-P ceramic biodegradation should be higher than cortical or cancellous bone.[22] A previous study suggested that OCP stimulates osteogenesis by osteoblastic cells and/or committed osteoprogenitors in rat calvarial periosteum.[23]

OCP may provide a site for osteoblastic cell recruitment and/or differentiation of mesenchymal stem cells into osteoblasts. It has been confirmed that serum constituents are selectively adsorbed onto synthetic OCP shortly after its implantation on mouse calvaria.[24] These serum constituents are glycoconjugates recognized by Maclura pomifera agglutinin (MPA) lectin and appear to be α2-HS glycoprotein based on their molecular weight and affinity for Ca ions.[24] MPA is known to bind to specifc sugar residues, such as α-D-galactose,[25] and its binding to glycoconjugates was previously detected in the primary bone extracellular matrix in both intramembranous and endochondral ossification.[26] α2-HS glycoprotein has been shown to induce the expression of alkaline phosphatase in epiphysial growth plate chondrocytes,[27,28] and to bind to Ca-P crystals, including OCP.[29] Furthermore, it has been indicated that OCP might be the suitable molecule for the absorption of growth factors such as recombinant bone morphgenetic proteins.[30] The ability of OCP implantation to enhance bone formation in bone marrow suggests that synthetic OCP provides a suitable scaffolding site for osteoblasts and/or osteoprogenitor cells that exist in the marrow space.

TRAP positive reactions were detetcted on the OCP and newly formed bone from 4 weeks after the implantation and strong TRAP reactions were detected on the OCP and bone at 6 weeks. Ultrastructural study indicated that these cells attached on the bone surface were osteoclasts, characterized by well-developed clear zones and ruffled borders. As reported previously,[31,32] the ruffled border consist of finger-shaped and plate-type cell processes. The cells on the implanted OCP attached by clear zone to OCP and developed several cell projections against OCP. As the OCP facing to the ruffled border was frayed and less electron dense, which indicated the active resorption of implanted OCP in this region, these multinucleated giant cells might be osteoclasts. However, the ultrastructure of cell projections in ruffled border did not showed the finger- or plate-shaped projections. Immunocytochemical studies indicated the localization of vacuolar H^+-ATPase and several types of proteinases at ruffled border and resorbing bone area.[33,34] Recent studies also showed that the different expressions of degrading enzymes of bone matrix by osteoclasts in endochondral and intramembranous bones.[35,36] These results suggest the functional heterogeneity of osteoclasts

by the resorbing calcified tissues and the structure of cell processes in ruffled border might be regulated by the resorbing materials by osteoclasts. Further studies are necessary to identify the ultrastructural and functional details of cell projections in the ruffled border of osteoclasts facing to implanted OCP.

Finally, OCP is a precursor of biological apatite in bone and teeth and synthetic OCP cannot be sintered and easily produced due to thermal dehydration.[37,38] It might be effective for synthetic OCP to be mixed with collagen and/or various synthetic polymers for the application to the bone defects in patients.

References

1) Termine JD, Eanes ED, Greenfield DJ, Nylen MU, Harper RA: Hydrazine-deproteinated bone mineral. Physical and chemical properties. Calcif Tissue Res, **12**: 73–90, 1973
2) Aoba T, Moreno EC: Changes in the nature and composition of enamel mineral during procine amelogenesis. Calcif Tissue Int, **47**: 356–364, 1990
3) Kim HM, Rey C, Glimcher MJ: Isolation of calcium-phosphate crystals of bone by non-aqueous methods at low temperature. J Bone Miner Res, **10**: 1589–1601, 1995
4) Simmer JP, Fincham AG: Molecular mechanisms of dental enamel formation. Crit Rev Oral Biol Med, **6**: 84–108, Review, 1995
5) Cheng PT: Formation of octacalcium phosphate and subsequent transformation to hydroxyapatite at low supersaturation: a model for cartilage calcification. Calcif Tissue Int, **40**: 339–343, 1978
6) Suzuki O: Interface science in formation of biominerals and biolecules. Clin Calcium, **14**: 9–15, Review, Japanese, 2004
7) Nelson DG, Barry JC: High resolution electron microscopy of nonstoichiometric apatite crystals. Anat Rec, **224**: 265–276, Review, 1989
8) Brown WE, Eidelman N, Tomazic B: Octacalcium phosphate as a precursor in biomineral formation. Adv Dent Res, **1**: 306–313, 1987
9) Boskey AL:Biomineralization: conflicts, challenges, and opportunities. J Cell Biochem Suppl, **30–31**: 83–91, Review, 1998
10) Chickerur NS, Tung MS, Brown WE: A mechanism for incorporation of carbonate into apatite. Calcif Tissue Int, **32**: 55–62, 1980
11) Siew C, Gruninger SE, Chow LC, Brown WE: Procedure for the study of acidic calcium phosphate precursor phases in enamel mineral formation. Calcif Tissue Int, **50**: 144–148, 1992
12) Bucholz RW: Nonallograft osteoconductive bone graft substitutes. Clin Orthop Relat Res, **395**: 44–52, 2002
13) LeGeros RZ: Properties of osteoconductive biomaterials: calcium phosphates. Clin Orthop Relat Res, **395**: 81–98, Review, 2002
14) Ogose A, Hotta T, Kawashima H, Kondo N, Gu W, Kamura T, Endo N: Comparison of Hydroxyapatite and beta tricalcium phosphate as bone substitutes after excision of bone tumors. J Biomed Mater Res B Appl Biomater, **72**: 94–101, 2005
15) Kamakura S, Sasano Y, Shimizu T, Hatori K, Suzuki O, Kagayama M, Motegi K: Implanted octacalcium phosphate is more resorbable than beta-tricalcium phosphate and hydroxyapatite. J Biomed Mater Res, **59**: 29–34, 2002
16) Hollinger JO, Kleinschmidt JC: The critical size defect as an experimental model to test bone repair materials. J Craniofac Surg, **1**: 60–68, 1990
17) Kamakura S, Sasano Y, Homma-Ohki H, Nakamura M, Suzuki O, Kagayama M, Motegi K: Multinucleated giant cells recruited by implantation of octacalcium phosphatase (OCP) in rat bone marrow share ultrastructural characteristics with osteoclasts. J Electron Microsc (Tokyo), **46**: 397–403, 1997
18) Sasano Y, Kamakura S, Nakamura M, Suzuki O, Mizoguchi I, Akita H, Kagayama M: Subperiosteal implantation of octacalcium phosphate (OCP) stimulates both chondrogenesis and osteogenesis in the tibia, but only osteogenesis in the parietal bone of a rat. Anat Rec, **242**: 40–46, 1995
19) LeGeros RZ: Preparation of octacalcium phosphate (OCP): a direct fast method. Calcif Tissue Int, **37**: 194–197, 1985
20) Tung MS, Brown WE: The role of octacalcium phosphate in subcutaneous heterotopic calcification. Calcif Tissue Int, **37**: 329–331, 1985
21) Suzuki O, Nakamura M, Miyasaka Y, Kagayama M, Sakurai M: Bone formation on synthetic precursors of hydroxyapatite. Tohoku J Exp Med, **164**: 37–50, 1991
22) Suzuki O, Kamakura S, Katagiri T: Surface chemistry and biological responses to synthetic octacalcium phosphate. J Biomed Mater Res B Appl Biomater, **77**: 201–212, Review, 2006
23) Sasano Y, Kamakura S, Homma H, Suzuki O, Mizoguchi I, Kagayama M: Implanted octacalcium phosphate (OCP) stimulates osteogenesis by osteoblastic cells and/or committed osteoprogenitors in rat calvarial periosteum. Anat Rec, **256**: 1–6, 1999
24) Suzuki O, Nakamura M, Miyasaka Y, Kagayama M, Sakurai M: Maclura pomifera agglutinin-binding glycoconjugates on converted apatite from synthetic octacalcium phosphate implanted into subperiosteal region of mouse calvaria. Bone Miner, **20**: 151–166, 1993
25) Kitajima I, Suganuma T, Murata F, Nagamatsu K: Ultrastructural demonstration of maclura pomifera agglutinin binding sites in the membranocystic lipodystrophy (Nasu-Hakola disease). Virchows Arch A Pathol Anat

Histopathol, **413**: 475–483, 1998
26) Schafer C, Heiss A, Schwarz A, Westenfeld R, Ketteler M, Floege J, Muller-Esterl W, Schinke T, Jahnen-Dechent W: The serum protein alpha 2-Heremans-Schmid glycoprotein/fetuin-A is a systemically acting inhibitor of ectopic calcification. J Clin Invest, **112**: 357–366, 2003
27) Ishikawa Y, Wu LN, Valhmu WB, Wuthier RE: Fetuin and alpha-2HS glycoprotein induce alkaline phosphatase in epiphyseal growth plate chondrocytes. J Cell Physiol, **149**: 222–234, 1991
28) Yang F, Schwartz Z, Swain LD, Lee CC, Bowman BH, Boyan BD: Alpha 2-HS-glycoprotein: expression in chondrocytes and augmentation of alkaline phosphatase and phospholipase A2 activity. Bone, **12**: 7–15, 1991
29) Honda M, Yoshioka T, Yamaguchi S, Yoshimura K, Miyake O, Utsunomiya M, Koide T, Okuyama A: Characterization of protein components of human urinary crystal surface binding substance. Urol Res, **25**: 355–360, 1997
30) Kamakura S, Sasano Y, Nakajo S, Shimizu T, Suzuki O, Katou F, Kagayama M, Motegi K: Implantation of octacalcium phosphate combined with transforming growth factor-beta1 enhances bone repair as well as resorption of the implant in rat skull defects. J Biomed Mater Res, **57**: 175–182, 2001
31) Akisa T, Miyaji T, Yoshida H, Inoue M: Ultrastructure of quick-frozen and freeze-substituted chick osteoclasts. J Ant, **190**(Pt 3): 433–445, 1997
32) Akisaka T, Yoshida H, Kogaya Y, Kim S, Yamamoto M, Kataoka K: Membrane modifications in chick osteoclasts revealed by freeze-fracture replicas. Am J Anat, **188**: 381–392, 1990
33) Nakamura H, Sato G, Hirata A, Yamamoto T: Immunolocalization of matrix metalloproteinases-13 on bone surface under osteoclasts in rat tibia. Bone, **34**: 48–56, 2004
34) Yamaza T, Tsuji Y, Goto T, Kido MA, Nishijima K, Moroi R, Akamine A, Tanaka T: Comparison in localization between cystain C and cathepsin K in osteoclasts and other cells in mouse tibia epiphysis by immunolight and immunoelectron microscopy. Bone, **29**: 42–53, 2001
35) Everts V, Korper W, Hoeben KA, Jansen ID, Bromme D, Cleutjens KB, Heeneman S, Peters C, Reinheckel T, Saftig P, Beertsen W: Osteoclastic bone degradation and the role of different cysteine proteinases and matrix metalloproteinases: differences between calvaria and long bone. J Bone Miner Res, **21**: 1399–1408, 2006
36) Everts V, Korper W, Jansen DC, Steinfort J, Lammerse I, Heera S, Docherty AJ, Beertsen W: Functional heterogeneity of osteoclasts: matrix metalloproteinases participate in osteoclastic resorption of calvarial bone but not in resorption of long bone. FASEB J, **13**: 1219–1230, 1999
37) Bigi A, Cojazzi G, Gazzano M, Ripamonti A, Roveri N: Thermal conversion of octacalcium phosphate into hydroxyapatite. J Inorg Biochem, **40**: 293–299, 1990
38) Honda Y, Kamakura S, Sasaki K, Suzuki O: Formation of bone-like apatite enhanced by hydrolysis of octacalcium phosphate crystals deposited in collagen matrix. J Biomed Mater Res B Appl Biomater, **80**: 281–289, 2007